JOURNAL OF MATERIALS SCIENCE 23 (1988) 3698–3705

Study by TEM, EDS, EELS and electron diffraction of precipitation reactions in a Cr–Mn austenitic steel with and without He-implantation

E. RUEDL
Commission of the European Communities, Joint Research Centre – Ispra Establishment, Materials Science Division, 21020 Ispra (VA), Italy

G. VALDRÉ
Dipartimento di Fisica and G.N.S.M.-C.N.R., University of Bologna, 40126 Bologna, Italy

A study of precipitation reactions in the Cr–Mn austenitic steel Nitronic 32 was performed by means of electron microscopy, electron diffraction, X-ray microanalysis and electron energy loss spectrometry. The material was examined: (a) after solution annealing and ageing at 773, 1023 and 1073 K; (b) after solution annealing followed by ambient temperature He-implantation and ageing at 773 and 1023 K and, (c) in the solution annealed state for comparison. The formation of the phases $M_{23}C_6$ and Cr_2N was observed. Their precipitation modes and sequence are described and discussed.

1. Introduction

Of the various possibilities offered by advancing technology for satisfying the increasing demand for energy, fusion energy in particular has attracted considerable interest.

The problems which determine the choice of materials to be used for the construction of a reactor structure are: safety, durability, reliability, waste disposal or recycling and cost.

A satisfactory solution of these problems imposes very stringent requirements on the material to be used. Despite this it is possible to envisage some potential categories of materials which might be suitable, one of which is the austenitic steels. We have explored some of the properties of these steels for use in a fusion reactor because of the large amount of background data available and the presumably lower cost as compared to vanadium alloys and silicon carbide. The latter two categories have the advantage of a lower intrinsic nuclear activation than steels, but, at present, there is insufficient technical knowledge to support their use in the construction of the complex structure of a fusion reactor.

Despite the large amount of data available on austenitic steels, there is still a shortage of knowledge on the behaviour of these materials in a fusion reactor when considering the physical and chemical operating conditions. The properties of the commercially available austenitic steels do not yet satisfy the requirements set by their use in the inner parts of a fusion reactor, which are the parts most exposed to radiation damage, activation, fatigue-creep, corrosion, etc.

With respect to activation it has recently been realized that the presence of impurities is a limiting factor for recycling [1]. If the impurity problem for recycling cannot be solved as a practical proposition, than at least Shallow Land Burial (SLB) is required. In any case some compositional modifications to the steel are necessary in order to allow SLB and to improve the operational performance.

According to the activation data available the amount of nickel present in austenitic steels should be reduced, or even completely replaced, by manganese. In this case, however, since the manganese is less stabilizing for the austenitic phase, the amount of carbon or nitrogen must be increased. As a consequence, phase instabilities and precipitation may take place on a larger scale at operational temperatures than occurs with conventional Cr–Ni austenitic steels.

The present work aims at the study of the structural properties of a commercial chromium–manganese steel (Nitronic 32). The composition of this material is interesting with regard to oxidation resistance [2] and mechanical properties, because of the high chromium and nitrogen contents. Precipitation phenomena in Cr–Mn steels have already been studied by several authors [3–12]. To our knowledge only preliminary investigations on Nitronic 32 have been reported [13]. They describe the precipitation produced by thermal ageing; here we report on an additional study of the effect of ageing on unirradiated material as well as on α-particle implanted samples. This latter aspect is of relevance in the fusion reactor where large quantities of helium are produced by (n, α) reactions in the structural materials. No basic information is available on the type of lattice damage produced by α-particle bombardment and on the effects of helium on the properties of Cr–Mn austenitic steels. It should be

0022–2461/88 $03.00 + .12

pointed out that the results presented here are related to a quite low displacement damage compared to fusion reactor damage levels, nevertheless the displacement rate is of the order of magnitude as expected in reactors based on magnetic confinement.

The examinations were performed by TEM, SEM, EDS, EELS and electron diffraction.

2. Experimental method

The Nitronic 32 steel examined in the present work was supplied by Armco Steel Corporation in the form of a hot rolled bar having the following composition: Cr 18 wt%, Mn 12.36%, Ni 1.54%, Si 0.54%, Cu 0.18%, Mo 0.15%, V 0.06%, Ti 0.005%, N 0.35%, C 0.11%, P 0.023%, O 0.007%.

2.1. Preparation of specimens

2.1.1. Solution annealed specimens

Discs of 3 mm diameter and $\sim 100\,\mu m$ thickness were prepared from the bar by slicing, punching and mechanical polishing. The discs were solution annealed in argon-filled silica capsules at 1373 K for 1/2 h and subsequently water quenched. Specimens for TEM were obtained by jet electropolishing.

2.1.2. Aged specimens

The discs were aged after solution annealing (a) at 773 K for 1000–2000 h, (b) at 1023 K for 2, 25 and 50 h and (c) at 1073 K for 100 h and prepared for TEM as described above. Carbon films were deposited on both sides of the aged samples which were immersed in a bromine–methanol solution; this dissolves the metal and leaves the precipitates formed by ageing. Such specimens were used for the analysis of single particles to avoid any interference with the surrounding matrix.

2.1.3. He-implanted and aged specimens

Discs of $\sim 150\,\mu m$ thickness were uniformly implanted with helium at a concentration of 500 a.p.p.m. by a 38 MeV α-particle bombardment at 310 ± 5 K in the Ispra cyclotron (use of an energy degrader wheel). The total dose in the samples corresponded to ~ 0.1 dpa and the displacement rate was $\sim 10^{-6}$ dpa sec^{-1}. After implantation the discs were annealed at 773 K for 2000 h, and at 1023 K for 2, 25 and 50 h and jet electropolished for TEM.

2.2. Instruments used

The samples were studied primarily by means of a Philips EM 400 T electron microscope equipped with a field emission gun, an EDAX EDS spectrometer and a GATAN spectrometer for EELS analysis and a JEOL 200 CX electron microscope. SEM observations were also carried out.

3. Results

3.1. Effects of ageing treatment

3.1.1. Precipitation at grain boundaries

The study of solution annealed specimens showed a fully austenitic structure with the grain boundaries free of precipitates. After ageing at 773 K and 1023 K, for all given ageing times, particles were observed at the grain boundaries and at the incoherent twin boundaries which were characterized by electron diffraction and EELS analysis (Figs 1a and b) and were identified as $M_{23}C_6$ carbides. At 773 and 1023 K the $M_{23}C_6$ particles formed and grew at well separated intervals, but their density and morphology were sensitive to the grain boundary orientation. At the incoherent twin boundaries the carbides grew into the matrix in the form of laths (Fig. 2). Ageing at 1073 K led to the formation of large plates of $M_{23}C_6$, even at the coherent twin boundaries. All these observations are consistent with earlier results of $M_{23}C_6$ precipitation in austenitic Cr–Ni steels [14–19]. The carbides were rich in chromium, but also contained iron and manganese and small amounts of nickel and molybdenum. Occasionally a very small amount of titanium and vanadium was also detected. The chromium content of the carbides increased with the time and temperature of annealing. Their mean composition after ageing at 1073 K was Cr 72 wt%, Fe 20%, Mn 7%, Mo $\lesssim 0.5\%$, Ni $\lesssim 0.5\%$ (normalized to 100).

3.1.2. Precipitation within the grains

3.1.2.1. General precipitation. A small number of

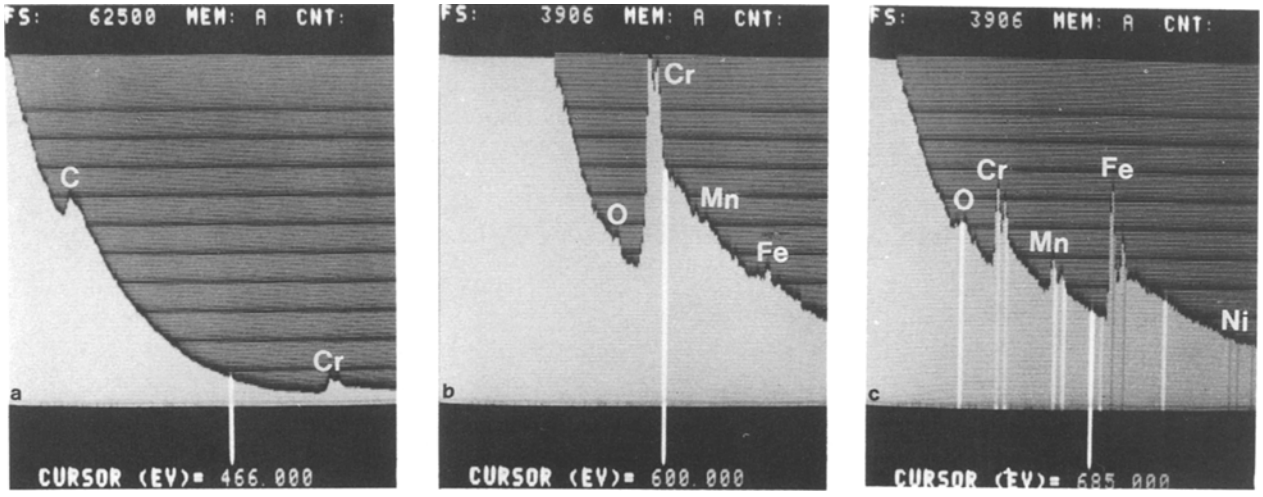

Figure 1 EELS spectrum obtained from $M_{23}C_6$ grain boundary particle in Nitronic 32 aged for 100 h at 1073 K. (a) at low magnification to show chromium and carbon edges, (b) enlarged at an intermediate range of energies to show the presence of manganese and iron, and (c) obtained from the surrounding matrix, for comparison.

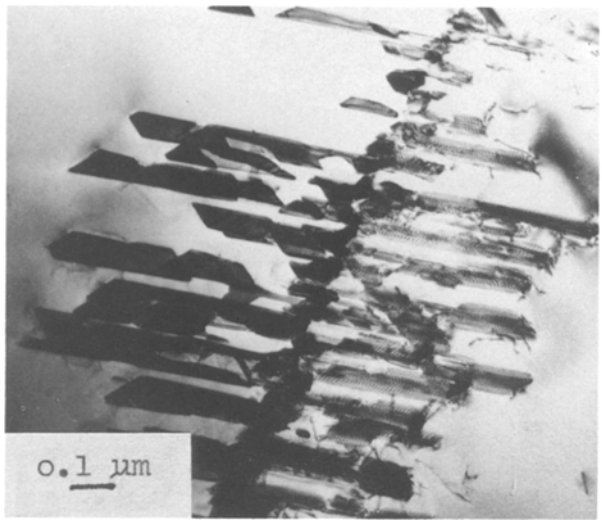

Figure 2 TEM micrograph of $M_{23}C_6$ particles in the form of laths at an incoherent twin boundary in Nitronic 32 aged for 100 h at 1073 K.

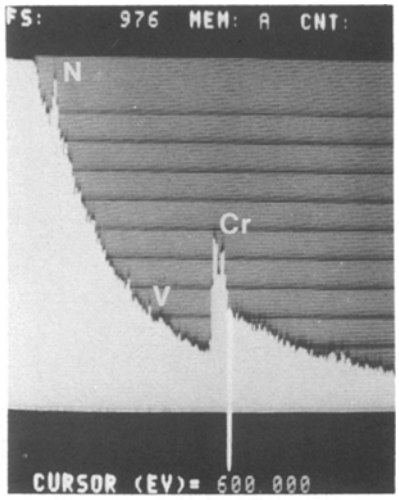

Figure 4 Typical EELS spectrum obtained from intragranular Cr_2N particles in Nitronic 32 aged for 100 h at 1073 K.

intragranular inclusions were present in solution annealed samples. EDS examination showed these inclusions to consist of MnS in which case they were a few micrometres in size, or of oxides of complex composition having a diameter of 50–100 nm. Ageing at 773 K and 1023 K up to 50 h did not lead to the formation of intragranular precipitates.

After ageing at 1073 K for 100 h, a number of additional particles were observed within the grains. These precipitates were predominantly of lenticular shape but also exhibited other morphologies, (Fig. 3). Dislocations and stacking faults emanated from them. An analysis by EELS showed that the particles contained chromium, nitrogen and a small amount of vanadium (Fig. 4). X-ray microanalysis also indicated the presence of a few wt % of iron.

Diffraction patterns obtained from these precipitates could be interpreted in terms of simple h c p unit cell indices with $a = 0.28$ nm, $c = 0.45$ nm and $c/a = 1.6$ and also in terms of h c p superlattice unit cell indices with $a = 0.48$ nm, $c = 0.45$ nm and $c/a = 0.937$. According to these data the precipitates formed at 1073 K were identified as Cr_2N.

The Cr_2N particles exhibited a complex contrast behaviour at their interface with the matrix. The contrast corresponded to thickness fringe contrast or to effects produced by the curvature of the lenticular particles [20]. Displacement fringe contrast was also observed due to the strong volume increase connected with Cr_2N formation. A high number of interfacial dislocations were also present. Selected area diffraction patterns obtained from the Cr_2N and the surrounding matrix showed mainly the following structural relationship

$$(0001)_{Cr_2N} \parallel (1\bar{1}1)_{fcc},\ (01\bar{1}0)_{Cr_2N} \parallel (\bar{2}\bar{1}1)_{fcc}$$

and

$$(2\bar{1}\bar{1}0)_{Cr_2N} \parallel (011)_{fcc}$$

in terms of simple h c p unit cell indices (Fig. 5). Other types of structural relationships were also observed however. Sometimes small inclusions were found

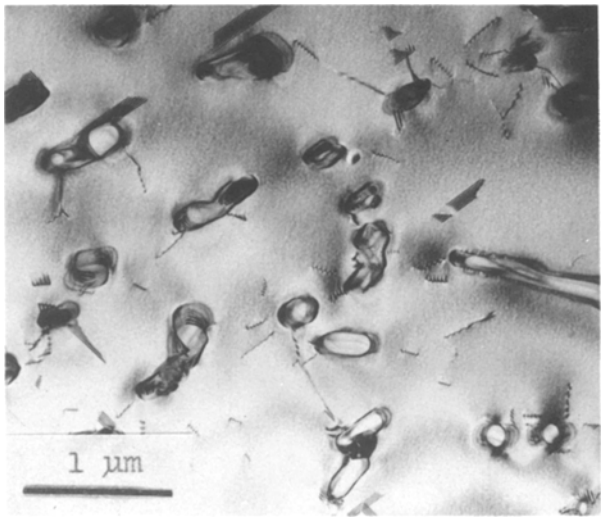

Figure 3 TEM micrograph obtained from Nitronic 32 aged for 100 h at 1073 K showing intragranular Cr_2N particles of various morphologies which exhibit complex interface contrast.

Figure 5 Selected area diffraction pattern obtained from the Cr_2N particles shown in Fig. 3. Basal (0001) h c p plane of Cr_2N in contact with (111) f c c matrix plane. Weaker spots are superlattice reflections; satellite spots are due to double diffraction.

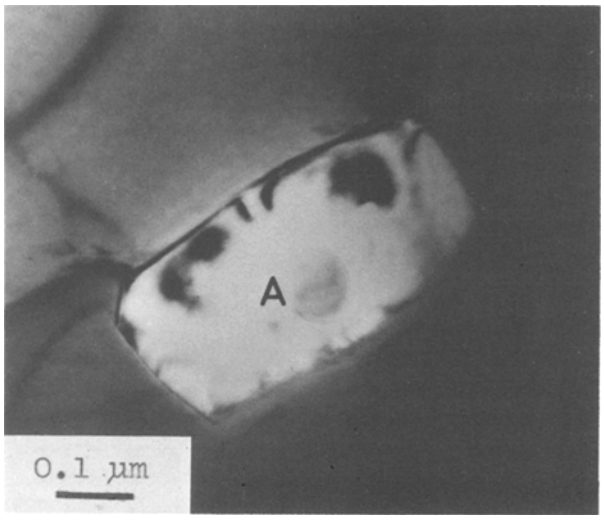

Figure 6 TEM micrograph of a Cr_2N particle in Nitronic 32 aged for 100 h at 1073 K showing a small oxide inclusion A acting as a nucleation centre.

inside the Cr_2N particles (Fig. 6). An analysis by EELS and EDS showed that the small inclusions, which acted as nucleation sites, coresponded to the small oxide particles present in the solution annealed material. The composition of this oxide, presumably of spinel type, was complex including mainly aluminium, manganese, chromium and iron but also some nickel and vanadium (Figs 7 and 8).

Beside the Cr_2N, intragranular, cube-shaped $M_{23}C_6$ was also detected after ageing at 1073 K.

3.1.2.2. Cellular precipitation. In a few samples (~20% of the total examined) a precipitation in the form of lamellae was observed after ageing at 1023 K for 25 and 50 h and at 1073 K for 100 h (Fig. 9). 10 to 20% of the grains in each of these samples was involved in this kind of precipitation. Sometimes the lamellae filled in the whole grain. In other cases the growth of the lamellae stopped even when a large part of the grain remained untransformed. Electron diffraction analysis indicated that the matrix alternating with the precipitate lamellae retained the austenitic

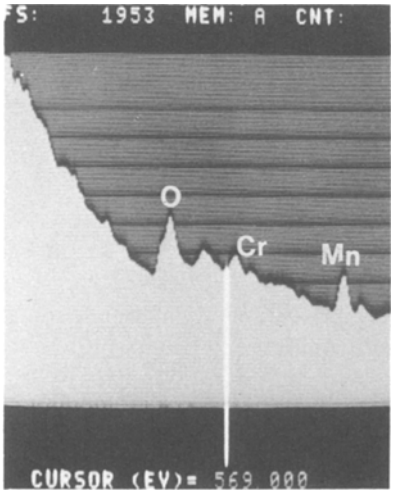

Figure 7 EELS spectrum from the small oxide inclusion A in the Cr_2N particle shown in Fig. 6.

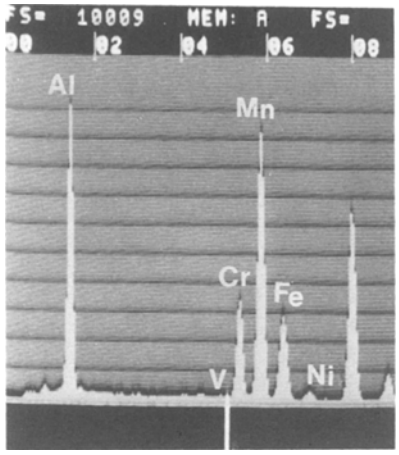

Figure 8 EDS spectrum from the small oxide inclusion A in the Cr_2N particle shown in Fig. 6. Cursor set at 5.4 keV.

structure despite a reduced nitrogen and carbon content; this is presumably due to a simultaneous chromium-loss (up to 4 wt %) and an increase of the manganese concentration. The lamella–matrix interfaces were incoherent. EDS and EELS analyses, as well as electron diffraction, showed that most of the lamellae contained chromium and nitrogen and had an h c p structure corresponding to Cr_2N. Some lamellae had chromium and carbon as major constituents, but also included iron and manganese and corresponded to f c c $M_{23}C_6$. Therefore the cellular precipitation consisted of colonies of lamellae of austenite alternating with lamellae of Cr_2N or $M_{23}C_6$.

3.2. Effects of ageing after α-particle bombardment

3.2.1. Precipitation at grain boundaries

No noteworthy difference was found in the formation of precipitates at the grain boundaries aged with or without helium implantation. The only phase formed after α-particle bombardment followed by ageing was $M_{23}C_6$. A zone denuded of clusters produced by the irradiation was visible after ageing at 773 K on both

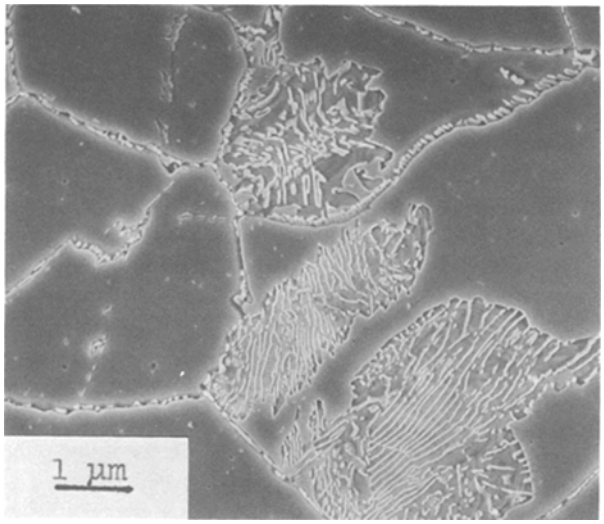

Figure 9 Secondary electron SEM micrograph of Nitronic 32 aged for 50 h at 1023 K showing cellular precipitation in some grains in the form of colonies consisting mainly of Cr_2N but also of $M_{23}C_6$ lamellae.

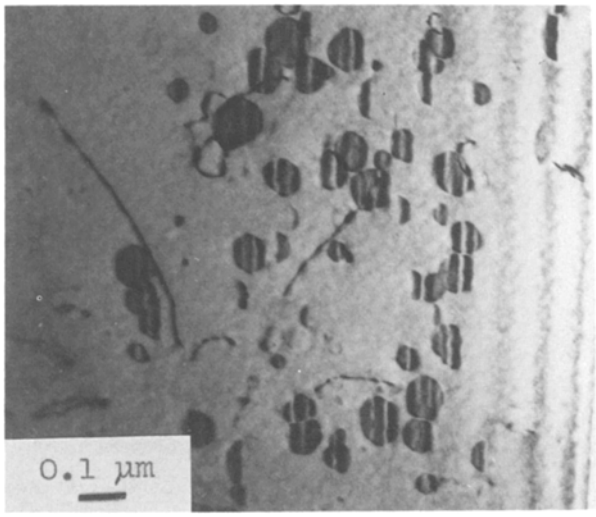

Figure 10 TEM micrograph of Frank interstitial dislocation loops present in He-implanted Nitronic 32 after ageing for 2 h at 1023 K.

sides of the boundaries. At this temperature no formation of intergranular helium bubbles was observed. Helium bubbles, however, were formed during ageing at 1023 K at some of the interfaces of the grain boundary carbides and in the spacing between them.

3.2.2. Precipitation within the grains

Annealing of the α-particle bombarded samples at 773 K for 2000 h led to the formation of a high density of defect clusters, many of them resolvable as dislocation loops. When the samples were annealed at 1023 K for 2 h, Frank interstitial dislocation loops were observed (Fig. 10). After ageing for 25 h at this temperature the number of Frank loops was somewhat reduced whereas the remainder had grown slightly. As shown in Fig. 11, particles were precipitated on the interstitial loops near the grain boundaries and helium bubbles of 50 to 100 nm diameter were observed between the precipitates, predominantly attached to dislocations.

After 50 h of ageing at 1023 K, the precipitates were seen throughout the grains. EELS (Fig. 12) and electron diffraction analyses indicated that they consisted mainly of Cr_2N but some $M_{23}C_6$ could also be identified. No cellular precipitation was detected in any of the specimens aged after helium-implantation (six samples).

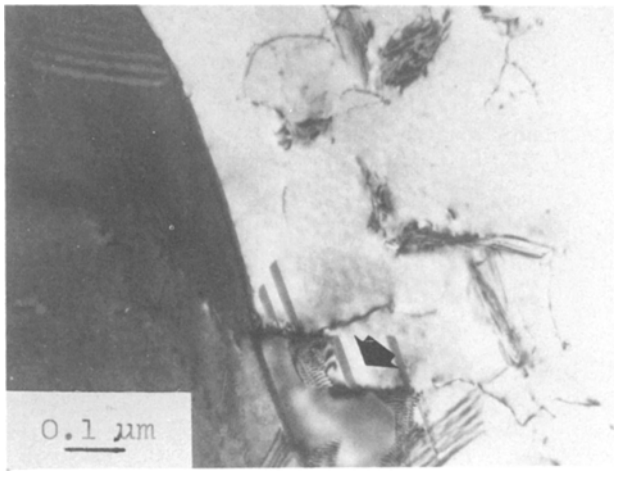

Figure 11 TEM micrograph of Cr_2N particles formed by heterogeneous nucleation on Frank dislocation loops near grain boundaries in He-implanted Nitronic 32 aged for 25 h at 1023 K. Large carbide particle at grain boundary indicated by arrow.

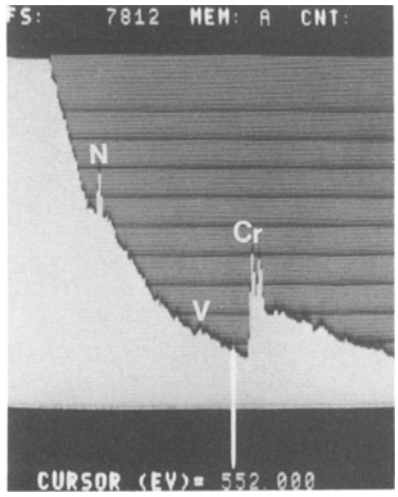

Figure 12 EELS spectrum from intragranular Cr_2N particles formed on Frank dislocation loops in He-implanted Nitronic 32 aged for 25 h at 1023 K as shown in Fig. 11.

4. Discussion

4.1. Phases formed in solution annealed samples

Solution annealed and rapidly cooled Nitronic 32 contains carbon and nitrogen in concentrations far above the solubility limit. Since the amount of strong MC forming elements such as titanium and vanadium in the material examined is very small and there is no niobium, the supersaturated carbon is precipitated on ageing in the form of $M_{23}C_6$, the carbide phase usually also observed in the Fe–Cr–Ni–C system [18]. The $M_{23}C_6$ formed in Nitronic 32 is chromium rich, but also accommodates iron, manganese, molybdenum, nickel and the impurity elements vanadium and titanium.

The supersaturated nitrogen on the other hand, precipitates in the form of chromium-nitride. The formation of a chromium-nitride compound can be expected since there is a decreasing stability of binary nitrides from Cr–Mn–Fe–Co–Ni as reported by Goldschmidt [21]. The question arises as to why in the austenitic matrix of Nitronic 32 h c p Cr_2N forms and not f c c CrN since the heat of formation of these two compounds is very similar [22]. Previous studies of nitrogen alloyed Cr–Mn steels of chromium contents in the range from ~ 16 to 23 wt % and nitrogen contents of up to 0.7 wt % have consistently shown that the precipitating phase is Cr_2N (see e.g. [4, 6–8, 10]). The same observations were made in the case of nitrogen alloyed Cr–Ni and molybdenum bearing Cr-Ni steels of similar chromium content [23–26]. Since no systematic equilibrium studies exist to our knowledge for the Fe–Cr–Mn–N system, the data reported in reference [27] referring to the system Fe–Cr–N are taken as a basis for thermodynamical considerations. In such alloys CrN is stable only up to chromium contents of ~ 10 wt % at 1073 K. A study of the equilibrium diagram of 18Cr–Fe–Ni–N alloys

[28] indicates that in AISI austenitic steels, at 1173 K, the equilibrium is between austenite and Cr_2N. Moreover Goldschmidt showed that in the Cr–N system Cr_2N is only stable at lower nitrogen contents and that a transformation to CrN occurs when the nitrogen content is significantly increased [29]. These arguments lead us to suggest that in Nitronic 32 the formation of Cr_2N is favoured with respect to CrN because of its relatively high chromium and low nitrogen content. Structural considerations lead to the same conclusion. A comparison of the lattice spacings of Cr_2N and CrN with those of the matrix shows that the misfit across the close-packed planes and in the close-packed directions, considerable for both compounds, is larger in the case of CrN. Finally, recent EELS quantitative analyses confirm that the composition of the precipitates corresponds to Cr_2N. The absence of the carbide M_6C and of the phases sigma, chi and Fe_2Mo does not exclude the possibility that these phases are formed in Nitronic 32. These compounds are thermodynamically stable in the Fe–Cr–Ni–Mo–C system [17, 18], but their formation is sluggish and controlled by various elements. Very little data are available on the formation of these phases in the Fe–Cr–Mn–C–N system. Recently it has been shown that the chi phase forms in a 10Cr–17Mn–0.1C–0.2N austenitic steel when 1.5 wt % Mo are added [13]. For a definite conclusion long duration tests would be required.

4.2. Microstructural evolution during ageing of solution annealed samples

The precipitation pattern of $M_{23}C_6$ and Cr_2N in Nitronic 32 is complex. Published data [23, 30] show that the free enthalpy change (negative for both reactions, is considerably greater for $M_{23}C_6$ formation. To obtain the effective driving energy for the formation by homogeneous nucleation, strain and surface energy factors must also be taken into account [31]. The strain energy associated with the formation and growth of these two compounds is positive, the increase being larger for Cr_2N. The strain energy however also depends on the state of coherency of the particle–matrix interface. A breakdown of coherency is possible and several mechanisms could be responsible for it. The strain due to volume increase can also be somewhat accommodated when the precipitate is nucleated at a high-energy interface. An estimate of the effective strain energy is therefore difficult.

The surface energy, which also reduces the driving energy for precipitation, is larger in the case of Cr_2N because of the considerable lattice misfit, already mentioned in Section 4.1., between the h c p Cr_2N and the f c c matrix. It is more difficult for the Cr_2N particles to develop low energy interfaces with the matrix than $M_{23}C_6$ in accordance with the present observations and those in reference [10]. One can therefore expect that the formation of $M_{23}C_6$ is more likely than that of Cr_2N in Nitronic 32. This is confirmed by the experimental observations.

The first phase which forms in solution annealed Nitronic 32 on ageing at 773, 1023 and 1073 K is $M_{23}C_6$. Since the grain boundaries are rapidly occupied by carbides, the nitrogen is precipitated as Cr_2N within the grains. This precipitation reaction is sluggish and occurs heterogeneously if possible, but otherwise homogeneously. Oxide inclusions of spinel type, present in the solution annealed state, represent suitable nucleation centres. Another type of heterogeneous Cr_2N nucleation will be discussed in Section 4.3.

The precipitation sequence described above does not hold in the case of cellular precipitation. This type of precipitation in Cr–Mn austenitic steels was examined by several authors some time ago [3, 4, 6, 32, 33]. They concluded that it takes place at some C/N ratios, at high temperatures, long ageing and is favoured by lattice strains. The cellular precipitation starts at grain boundaries and rapidly propagates into one of the grains. More recently a systematic study of cellular precipitation was made on Cr–Ni alloys with nitrogen levels ranging from ~ 0.4 to ~ 0.6 wt % [34–36]. These latter authors point out that the features of cellular growth in alloys containing both substitutional and interstitial solutes are different from the cellular precipitation pattern in binary solute alloy systems and concluded that long range nitrogen diffusion is important. Direct evidence for diffusion of nitrogen over long distances in grains exhibiting cellular Cr_2N formation was recently obtained for a Cr–Ni–N steel by X-ray microanalysis [37].

4.3. Microstructural evolution during ageing of α-particle bombarded samples

The main sources of helium production in the bulk of structural materials in the fusion reactor are the (n, α) reactions. Since intense, high energy neutron sources do not yet exist, for the study of the effects of helium on the behaviour of structural materials, the helium must be produced in other ways. The methods available, their advantages and their disadvantages are discussed in reference [38]. The high energy α-particle bombardment of samples in a cyclotron, as carried out in the present work, rapidly produces large amounts of helium in a sample without excessive activation. Moreover the samples are damaged at a displacement rate prevailing in the first wall of a fusion reactor based on magnetic confinement and the local lattice damage produced is the same as that created by (n, α) helium atoms. As such, the helium implantation technique employing a cyclotron provides a useful simulation for damage produced by α-particles in a fusion reactor. Though such samples may be used to study the effects of helium on the microstructural evolution, it must be borne in mind that the accumulated displacement damage is quite low and the introduction rate of helium is much higher than the helium production rate in the first wall of a fusion reactor. A sufficiently high displacement damage could be obtained by a dual beam bombardment, a method not available at the Ispra Centre. This method, however, suffers from an excessively high displacement rate and may alter the results due to the additionally implanted heavy ions coming to rest in interstitial positions.

In the as α-bombarded Nitronic 32 samples no formation of precipitates was observed. Since the total

displacement damage produced by the α-bombardment was only ~0.1 dpa, the conditions for the formation of precipitates during the bombardment were apparently not fulfilled [39]. When the samples of Nitronic 32, α-implanted at room temperature are subsequently aged, the relative low density of free point defects produced by the bombardment presumably anneals out very rapidly while a dislocation structure is formed. This structure consists after the 2000 h annealing at 773 K, of a high density of very small dislocation loops. The larger loops present in a somewhat lower number after annealing at 1023 K for 2 h, were of interstitial type containing a stacking fault (Frank loops). These loops were relatively stable on annealing. Possible reasons for such a behaviour could be a low stacking fault energy of Nitronic 32 or difficulties in nucleating Shockley partials to eliminate the extrinsic fault. It could also be related to a strong nitrogen interstitial interaction [40].

Although the composition of the inserted (1 1 1) loop planes and of the surrounding faulted lattice is not known, an enhanced concentration of chromium or, more probably, of the small nitrogen atoms can be assumed in order to explain the nucleation of Cr_2N in their neighbourhood on longer ageing at 1023 K. It should be emphasized that no intragranular Cr_2N is formed when solution annealed samples are aged in the same conditions. The precipitation onto the Frank loops begins near the grain boundaries at a distance corresponding roughly to the width of the cluster-free zone described in Section 3.2.1. where the composition of the matrix is presumably most favourable for Cr_2N formation. After ageing at 1023 K for 50 h, the enhanced formation of precipitates on Frank loops extends to the centre of the grains, predominantly in the form of Cr_2N but also as $M_{23}C_6$. The precipitation of $M_{23}C_6$ on Frank loops was observed previously in the case of a He-injected or neutron irradiated AISI 316 steel containing boron [41].

The kinetics of intragranular Cr_2N formation is therefore different in α-implanted samples. The Cr_2N forms at a lower temperature and with shorter ageing times due to nucleation in the vicinity of the Frank interstitial loops, presumably as a consequence of local nitrogen segregation.

The absence of cellular precipitation in the samples aged after He implantation could possibly be due to the relaxation of lattice strains due to the α-bombardment. But there is another possible reason. Since the features of cellular growth do not show any significant difference in Cr–Ni and Cr–Mn austenitic steels, it can be assumed that long-range diffusion of nitrogen is also important for cellular growth in the latter materials. Since in the α-implanted samples on ageing a dislocation structure evolves and local nitrogen segregation occurs, the diffusion of nitrogen over longer distances may be difficult. Additional investigations are in progress on Nitronic 32 to confirm this assumption. Concerning the precipitation behaviour of helium in Nitronic 32, the present observations show that the injected helium is not yet mobile at 773 K. Annealing at 1023 K instead leads to the formation of He bubbles with the aid of thermal vacancies at grain boundaries and on some intergranular carbide–matrix interfaces depending on their state of coherency. No significant formation of He bubbles on the Cr_2N particles was observed although these particles develop mainly high energy interfaces. It is therefore assumed that longer annealing times or higher ageing temperatures are needed to move the helium by diffusion or bubble motion to the Cr_2N–matrix interfaces.

5. Conclusions

The conclusions are as follows.

(a) Ageing of solution annealed samples of the austenitic Cr–Mn steel Nitronic 32 leads at 773 K to the precipitation of $M_{23}C_6$ and at 1023 and 1073 K to the additional formation of Cr_2N. The precipitation reactions can occur in two different ways.

(i) Usually $M_{23}C_6$ forms first at high angle intergranular interfaces followed by a sluggish precipitation of Cr_2N within the grains. This sequence is expected on the basis of the greater free enthalpy change for $M_{23}C_6$ formation and the low driving energy for Cr_2N precipitation.

(ii) Occasionally a cellular precipitation is also observed in some grains, mainly in the form of colonies of Cr_2N lamellae but also of $M_{23}C_6$ lamellae alternating with matrix lamellae. Possible explanations for this type of precipitation could be a higher local nitrogen or carbon content than nominal and the presence of lattice strains in some grains.

(b) Ageing of solution annealed and ambient temperature α-implanted Nitronic 32 at 773 K leads to the formation of $M_{23}C_6$ and at 1023 K to the precipitation of $M_{23}C_6$ and Cr_2N as well as to the formation of He bubbles. No cellular precipitation was observed. The sequence of $M_{23}C_6$ and Cr_2N formation is similar to that observed for samples aged in the absence of helium with the $M_{23}C_6$ precipitating first. The intragranular formation of Cr_2N is however enhanced by its nucleation on Frank interstitial dislocation loops.

(c) The helium in α-implanted Nitronic 32 is not yet mobile at 773 K. At 1023 K it precipitates in the form of bubbles at high-energy interfaces and at dislocations within the grains.

(d) Cellular precipitation, deleterious for ductility and corrosion, can possibly be avoided by the following.

(1) An appropriate solution annealing and cooling treatment to obtain (a) a homogeneous distribution of carbon and nitrogen and (b) reduced lattice strains.

(2) Relieving the stresses by means of a low dose irradiation.

(3) Preventing long range nitrogen diffusion by means of an irradiation induced dislocation loop structure and local nitrogen segregation.

Acknowledgements

The authors are indebted to Professor U. Valdré for useful discussions and to Mr N. Waechter for the preparation of the α-implanted samples.

References

1. C. PONTI, *Fusion Technol.* **13** (1988) 157.
2. G. GESMUNDO, C. DE ASMUNDIS, G. BATTILANA

and E. RUEDL, *Werkst. Korros,* **38** (1987) 367.
3. C. M. HSIAO and E. J. DULIS, *Trans. Amer. Soc. Met.* **49** (1957) 655; *ibid.* **50** (1958) 773 and *ibid.* **52** (1960) 855.
4. G. HENRY and J. PLATEAU, *NML Tech. J.* **5** (1963) 25.
5. E. J. DULIS, *Iron and Steel Inst., London, Spec. Rept* **76** (1962) 87.
6. J. K. MUKHERJEE and B. R. NIJHAWAN, *J. Iron Steel Inst., London* **205** (1967) 62.
7. B. R. NIJHAWAN, P. K. GUPTE, S. S. BHATNAGAR, B. K. GUHA and S. S. DHANJAL, *ibid.* **205** (1967) 292.
8. R. CHOUBEY, K. PRASAD and T. BANERJEE, *Trans Indian Inst. Met.* **21** (1968) 9.
9. P. L. AHUJA, B. N. HALDER and S. S. BHATNAGAR, *J. Mater. Sci.* **6** (1971) 439.
10. K. MIELITYINEN-TIITTO, *Acta Polytechnica Scandinavica,* **CH141** (1979). pp. 1–69.
11. R. PRESSER and J. M. SILCOCK, *Met. Sci.* **17** (1983) 241.
12. A. H. BOTT, F. B. PICKERING and G. J. BUTTERWORTH, *J. Nucl. Mater.* **141–143** (1986) 1088.
13. E. RUEDL and T. SASAKI, *ibid.* **122** (1984) 794.
14. M. H. LEWIS and B. HATTERSLEY, *Acta Metall.* **13** (1965) 1159.
15. F. R. BECKITT and B. R. CLARK, *ibid.* **15** (1967) 113.
16. L. K. SINGHAL and J. W. MARTIN, *Trans. Met. Soc. AIME* **242** (1968) 814.
17. B. WEISS and R. STICKLER, *Metall. Trans.* **3** (1972) 851.
18. D. PECKNER and I. M. BERNSTEIN, "Handbook of Stainless Steels", McGraw-Hill, New York (1977).
19. N. TERAO and B. SASMAL, *Metallography* **13** (1980) 117.
20. H. HASHIMOTO, *Met. Phys.* **8** (1962) 100.
21. H. J. GOLDSCHMIDT, "Interstitial Alloys", (Butterworths, London, 1967) p. 229.
22. *Idem, ibid.* p. 221.
23. G. GRUETZNER, PhD Thesis, Rheinisch-Westfaelische Technische Hochschule, Aachen, FRG (1971).
24. G. GRUETZNER, *Stahl Eisen* **93** (1973) 9.
25. A. FREISSMUTH, *Berg- u. Huettenm. Mh.* **112** (1967) 197.
26. D. BLAZEJAK, G. HERBSLEB and K. J. WESTERFELD, *Werkst. Korros.* **27** (1976) 398.
27. Y. IMAI, T. MASUMOTO and K. MAEDA, *Sci. Rept. RITU A* **19** (1967) 21.
28. T. MASUMOTO and Y. IMAI, *J. Jpn Inst. Met.* **33** (1969) 1364.
29. H. J. GOLDSCHMIDT, "Interstitial Alloys", Butterworths, London (1967) p. 217.
30. F. D. RICHARDSON, *J. Iron Steel Inst., London,* **175** (1953) 33.
31. J. W. CHRISTIAN, "Theory of Transformations in Metals and Alloys", 2nd Edn (Pergamon, Oxford, 1975), Part I, p. 459.
32. K. J. IRVINE, D. T. LLEWELLYN and F. J. PICKERING, *J. Iron Steel Inst. London* **199** (1961) 153.
33. F. B. PICKERING, "Physical Metallurgy and the Designs of Steels", Applied Science Publishers, London (1978) Chap. 11.
34. M. KIKUCHI, S. K. CHOI, Y. OGURA and R. TANAKA, *J. Jpn Inst. Met.* **45** (1981) 683.
35. M. KIKUCHI, S. K. CHOI and R. TANAKA, in Proceedings International Conference on Solid-Solid Phase Transformations, (edited by H. I. Aaronson, D. E. Laughlin, R. F. Sekerka and C. M. Wayman, The Metallurgical Society of AIME, New York 1982) p. 969.
36. M. KIKUCHI, S. K. CHOI and R. TANAKA, *J. Mater. Sci. Soc. Jpn* **21** (1985) 358.
37. M. KAJIHARA, S. K. CHOI, M. KIKUCHI, R. TANAKA, Y. SEO, T. OKUMURA and Y. KONDOH, *Z. Metallkde* **77** (1986) 515.
38. H. ULLMAIER, *Nucl. Fusion* **24** (1984) 1039.
39. K. C. RUSSEL, *Prog. Mater. Sci.* **28** (1984) 414.
40. Y. KATANO, T. ARUGA and K. SHIRAISHI, *J. Nucl. Mater.* **132** (1985) 32.
41. K. SHIRAISHI, K. FUKAYA and K. FUKAI, *ibid.* **119** (1983) 268.

Received 7 August 1987
and accepted 28 April 1988